PAPER • **OPEN ACCESS**

Strength of notched Ti-6Al-4V specimens not subjected to solution treatment and over-aging under cyclic loading

To cite this article: E V Arcieri and S Baragetti 2023 *IOP Conf. Ser.: Mater. Sci. Eng.* **1275** 012022

Strength of notched Ti-6Al-4V specimens not subjected to solution treatment and over-aging under cyclic loading

E V Arcieri[1] and S Baragetti[1]

[1]Department of Management, Information and Production Engineering, University of Bergamo, Viale Marconi 5, Dalmine 24044, Italy

sergio.baragetti@unibg.it

Abstract. Ti-6Al-4V alloy is a popular titanium alloy due to its high strength / density ratio, high toughness, superior corrosion resistance and good biocompatibility. After forming operations, Ti-6Al-4V is typically subjected to Solution Treatment and Over-Aging (STOA). Fatigue is one of the most frequent causes of failure in mechanical components. The prediction and optimization of the strength of structural components under cyclic loads therefore plays a strategic role and must take into consideration the presence of defects. The aim of the work is to investigate the axial fatigue behaviour of Ti-6Al-4V alloy not subjected to STOA in inert environment in the presence of notches. The experimental results agree well with the results obtained using the Haigh diagram.

1. Introduction

Ti-6Al-4V titanium alloy is commonly adopted in the aeronautical, maritime and biomedical industries owing to its high strength / mass ratio, high toughness, high resistance to corrosive environments, and good biocompatibility [1-4].

Cyclic loading is a common cause of failure in the above-mentioned fields [5]. The structural integrity of the components must be guaranteed during their service under different loading and environmental conditions [6, 7], even in the presence of defects, which are caused by the production process or by the impact of objects. Some components are today produced by additive manufacturing techniques [8] which are feasible to produce complex geometries, even in titanium alloys. The poor surface quality obtained with these techniques contributes to the reduction of fatigue strength [9]. Even the conventional processes can induce defects that need to be monitored. Foreign objects can collide with the aircraft engine parts, frequently made of titanium alloys. The occurrence of high tensile stresses associated with the impact-damage may reduce service life [10, 11].

After forming operations, Ti-6Al-4V is commonly Solution Treated and Over-Aged (STOA), i.e. subjected to solution treatment and vacuum annealing [12]. The behavior of STOA-treated Ti-6Al-4V in inert and aggressive environments and under quasi-static and fatigue loads is presented in [13-17]. In [18, 19] the behavior of the Ti-6Al-4V alloy not subjected to the STOA treatment under quasi-static loading is described for different notches and different environments.

The aim of this work is to study the fatigue behavior of Ti-6Al-4V without STOA treatment in inert environment [20]. The lack of the treatment could reduce the manufacturing cost. Notched Ti-6Al-4V specimens not subjected to STOA were tested under cyclic axial loading, with a load ratio $R = 0$. The experimental results are in good agreement with those provided by the analysis using the Haigh diagram.

2. Materials and methods

Authors applied in this work the same research method adopted in past works on applications in different mechanical engineering sectors [21-24].

The geometry of the tested specimens is shown in Figure 1, where *d* is the depth of the notch. The following values of *d* were analyzed: 0.5, 1.0 and 2.0 mm. The chemical composition of the specimens is reported in Table 1 [14]. The Ti-6Al-4V alloy was not subjected to STOA, with a consequent small improvement in mechanical properties compared to the alloy subjected to STOA as shown in Table 2 [12, 13, 25, 26], where *UTS* indicates the ultimate tensile strength, *YS* the yield stress and *E* the Young's modulus. The STOA treatment applied to obtain the mechanical properties of Table 2 is solution treatment at 925 °C for 1 h and vacuum annealing at 700°C for 2 h. The notches of the specimens were created by milling at low cutting speed in order to induce low residual stresses. No stress relief was conducted after the production of the notches.

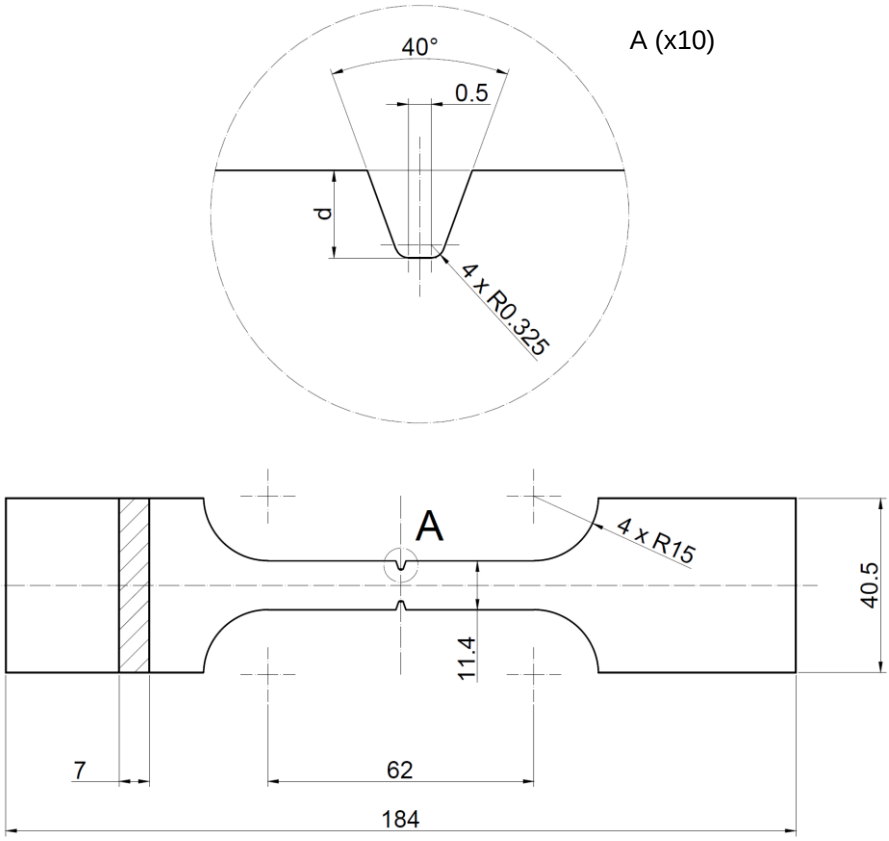

Figure 1. Geometry of the tested specimens.

Table 1. Chemical composition of Ti-6Al-4V (%wt.) [14].

Ti	Al	V	Fe	O	N	H	C
Bal.	5.97	4.07	0.20	0.19	0.05	0.015	0.003

Table 2. Mechanical properties of Ti-6Al-4V with and without STOA [12, 13, 25, 26].

	UTS (MPa)	*YS* (MPa)	*E* (MPa)	*v*
With STOA	947-990	900-945	110000	0.342
Without STOA	1000-1100	958-1050	110000	0.342

To determine the stress concentration factor *SCF* at the notch a plane stress linear elastic finite element analysis was performed on the model of a quarter of the specimens using the Abaqus Standard code [27], Figure 2 [28]. A homogeneous isotropic elastic material model was used for the analyses, with the properties of Table 2. Figure 2a shows the applied boundary and load conditions. Symmetry boundary conditions were implemented. A uniform load of 1 MPa was applied to the upper edge of the specimens. Figure 2b shows a detail of the mesh created at the notch. For each notched specimen, finite element model convergence was achieved in order to accurately capture the stress gradient at the notch. Figure 2c shows the resulting stress distribution, i.e. the stresses in the y direction according to the coordinate system in Figure 2a, for one of the investigated geometries, d = 2.0 mm.

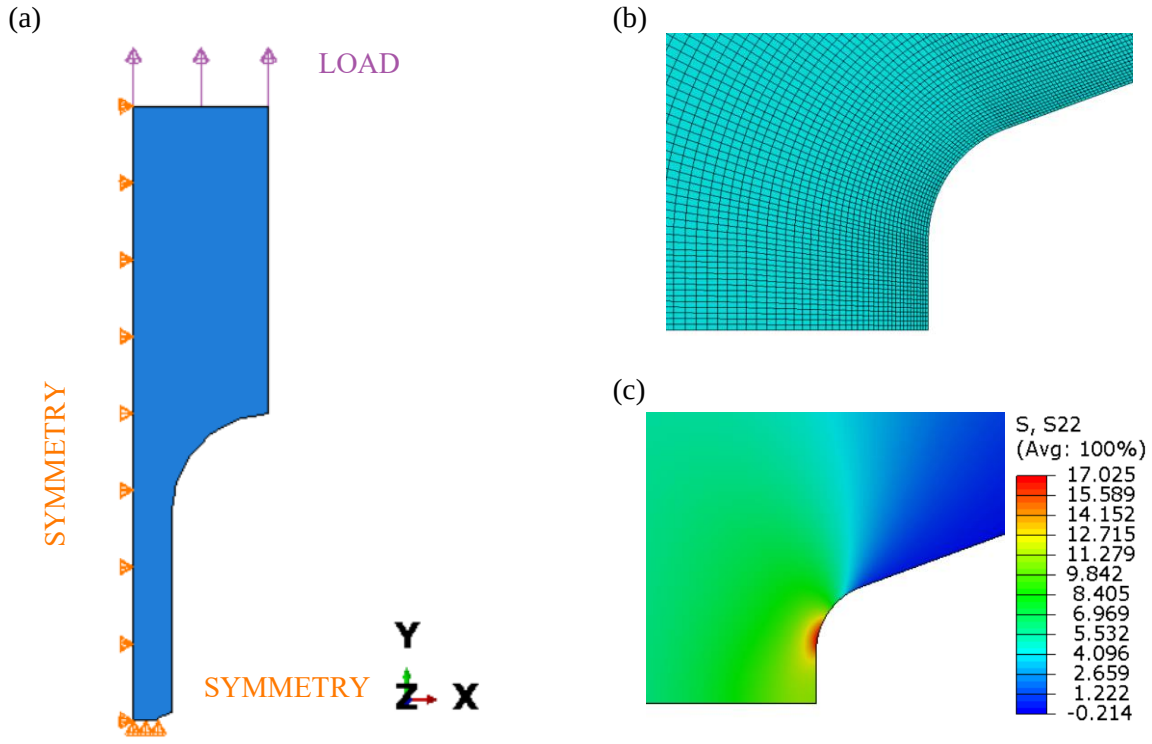

Figure 2. Finite element model for the determination of *SCF*: (a) boundary and load conditions, (b) mesh at the notch, (c) axial stresses at the notch (MPa) [28].

Before the experimental tests, the surface of the specimens, including the notch surface, was polished with grit paper and diamond paste. Fatigue axial tests were conducted with a frequency f = 5 Hz and a load ratio R = 0. The three specimens were tested in air environment, but a layer of insulating tape was placed adherent to the notches of the two specimens with d = 0.5 and 1.0 mm to simulate vacuum conditions. Another technique for simulating vacuum conditions is the application of beeswax or paraffin oil [15]. The fatigue tests were performed on the notched specimens according to the step loading procedure described by Nicholas in [29], which enables obtaining preliminary results in a fast way, similarly to the Locati method [30, 31]. The step loading procedure consists of the sequential implementation of load blocks on the specimen. In each load block, the specimen is subjected to N_{life} loading cycles, where N_{life} is the number of cycles at which the stress to failure must be determined. The load is incrementally increased in the following load blocks until the specimen fails, at a number of cycles N_{fail} less than or equal to N_{life}. According to Equation 1, the stress range σ_{SL} that causes the failure of the specimen after N_{life} loading cycles is determined as the linear interpolation between the stress range applied in the last unfailed load block, σ_{prev}, and the stress range applied in the load block in which the failure occurs, σ_{fail}:

$$\sigma_{SL} = \sigma_{prev} + \frac{N_{fail}}{N_{life}} \left(\sigma_{fail} - \sigma_{prev} \right) \quad (1)$$

The step loading procedure provides reliable results if the crack propagation is very fast in the experiments. Any crack propagation in previous load blocks could influence the results, as the specimen strength would be changed. The ideal would be to have the entire crack propagation phase in the load block in which the specimen fails [29].

3. Results and discussion

Table 3 shows the results of the analysis conducted in this work. F_{fail} is the axial load applied to the specimen in the load block in which the failure occurred in the experimental test, σ_H is the stress to failure (stress range) calculated using the Haigh (modified-Goodman) diagram and Δ is the discrepancy between the two admissible stress ranges σ_{SL} and σ_H. The reported stresses are nominal stresses referred to the net area of the specimens. The first specimen, with a notch depth of 0.5 mm, failed at a maximum load in the fatigue cycle of 17.0 kN after 135544 cycles applied in the last load block. The second specimen, with a 1.0 mm notch depth, failed at a maximum load in the fatigue cycle of 16.8 kN after 160650 cycles in the block. The third specimen, with a notch depth of 2.0 mm, failed in the first load block, when a maximum load in the fatigue cycle of 13.0 kN was applied; the failure occurred after 139458 cycles. The step loading methodology provides a stress range to failure of 220 and 248 MPa for the specimens with a notch depth of 0.5 and 1.0 mm respectively at a fatigue life of 200000 cycle. For the third specimen Equation 1 was not used because the specimen failed in the first applied load block. The stress range to failure for the specimen with the notch depth 2.0 mm is 251 MPa at a fatigue life of 139458 cycles [28]. The σ_H value was calculated according to the procedure illustrated in Figure 3. The figure is an example and refers to the case of the specimen with d = 0.5. The first step was the determination of the alternating stress to failure σ_a (N_{life}, R = -1) at the fatigue life N_{life} starting from the S-N (σ_a-N_{cycles}) curves for each notched specimen not subjected to STOA (Figure 3a). The S-N curves for the three notched specimens with the three corresponding values of stress concentration factor *SCF* were built taking into consideration the brittle behavior of the alloy observed in [19]. In the analysis it was assumed that the alternating stress to failure at a fatigue life of 1000 loading cycles corresponds to the stress which induces static failure, i.e. *UTS* / *SCF*. The alternating stress to failure at a fatigue life of 2 million cycles for the notched specimens was assumed to be 0.7 x 0.33 x *UTS* / *SCF* [28]. The average of the two *UTS* values reported in Table 2 for Ti-6Al-4V not subjected to STOA treatment was used to create the S-N curves. Given the σ_a (N_{life}, R = -1) value calculated in the first step, a Haigh diagram was built for each notched specimen. Even in this diagram the brittle behavior of the alloy observed in [19] was considered, dividing *YS* by *SCF* to define the yield line and *UTS* by *SCF* to define the fatigue limit curve (Goodman line). The yield domain is defined by the area between the vertical axis of the diagram, the horizontal axis, and the yield line. The failure domain is defined by the area between the vertical axis, the horizontal axis and the Goodman line. The intersection of these two domains provides the strength domain. By intersecting the curve corresponding to R = 0 with the limit curve of the strength domain, it is possible to identify the mean and alternating stresses to failure, $\sigma_{m,lim}$ (N_{life}, R = 0) and $\sigma_{a,lim}$ (N_{life}, R = 0) at the fatigue life N_{life} when the load ratio R is equal to 0. In all the three analysed cases, the failure domain is stricter than the yield domain. The sum of $\sigma_{m,lim}$ (N_{life}, R = 0) and $\sigma_{a,lim}$ (N_{life}, R = 0) is σ_H. The analysis with the Haigh diagram provides a stress range to failure of 268, 229 and 225 MPa for the tested specimens. The corresponding discrepancies Δ are 18%, 8% and 12%. Scatter is an intrinsic characteristic of fatigue properties of materials and components. The fatigue strengths of similar specimens or components subjected to the same fatigue load may be very different [32]. For this reason, it is possible that the repetition of the experimental tests provides slightly different results, with slightly different discrepancies compared with those reported in Table 3. Since all the values of discrepancies obtained in this work are less than 20%, they can be considered acceptable. The discrepancies may also be due to the assumptions made in the calculation including the absence of residual stresses after the creation of the notches. As known, residual stresses affect the fatigue life of

components [33]. Even if the results of the step loading procedure and the estimation of the stress to failure with the Haigh diagram are quite similar, further investigations are needed.

Table 3. Results of the experimental tests (data of the third specimen from [28]).

d (mm)	SCF	F_{fail} (kN)	N_{fail}	σ_{SL} (MPa)	σ_H (MPa)	Δ (%)
0.5	2.48	17.0	135544	220	268	18
1.0	2.91	16.8	160650	248	229	8
2.0	3.11	13.0	139458	251	225	12

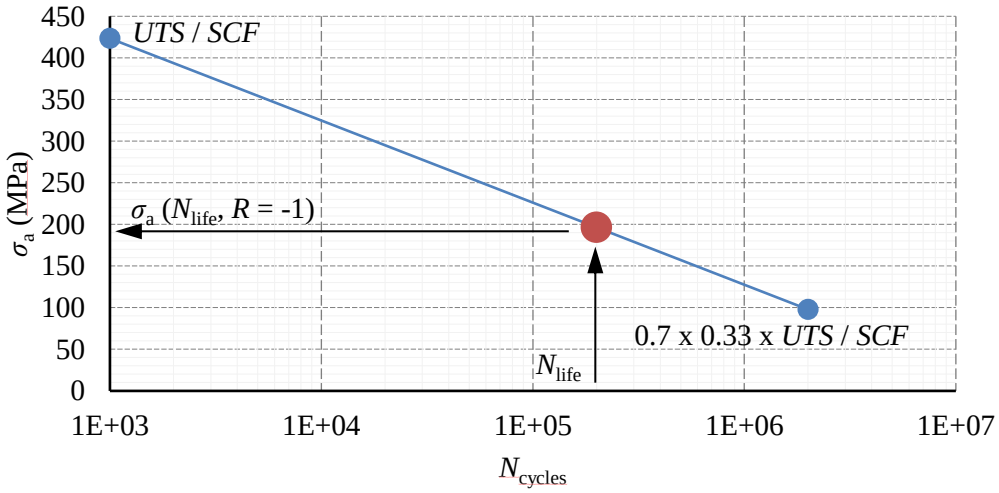

(a)

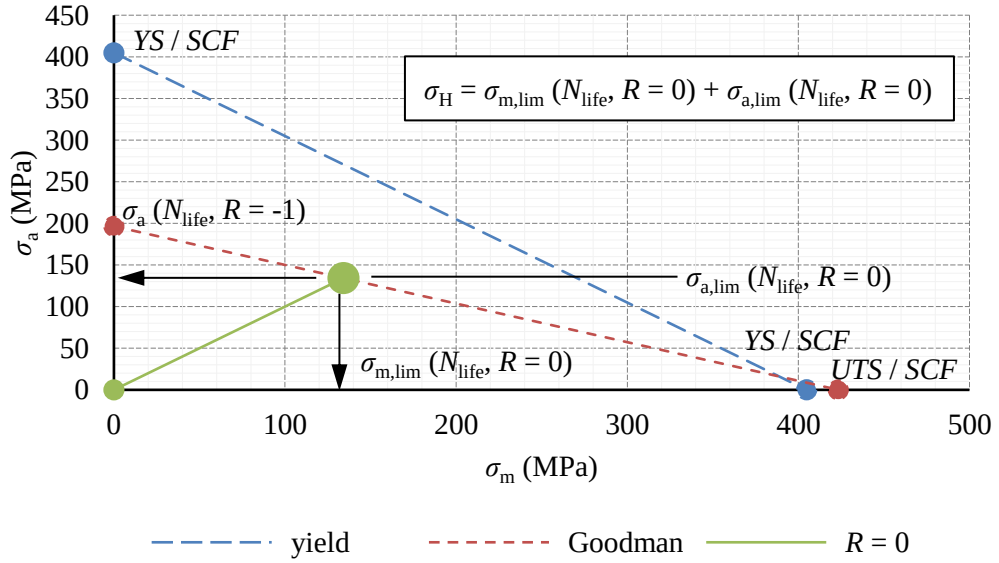

(b)

Figure 3. Calculation of σ_H: (a) S-N curve, (b) Haigh diagram.

Figure 4 shows the fracture surfaces of the tested specimens, observed with a stereo microscope. The nucleation areas are marked. In all the cases the fatigue cracks propagated from the notches due to the stress concentration induced by them. In the specimen with notch depth d = 0.5 mm, the crack nucleation area lies between a vertex of the fracture surface and the midplane of the specimen normal to the notch edge (Figure 4a). In the specimen with d = 1.0 mm, the crack propagated from a point between the two vertices of the fracture surface (Figure 4b). In the specimen with d = 2.0 mm, the crack propagated from the area close to one vertex of the fracture surface (Figure 4c, [28]). There are no symmetry planes in the three fracture surfaces. Only the fracture surface of Figure 4b tends to be symmetric, with the crack nucleation point quite equidistant from the vertices lying on one notch. In this area the theoretical stress state is plane stress. The general lack of symmetry in the fracture surface can be justified by possible mounting misalignments of the specimen with respect to the axis of the testing machine, presence of defects in the specimen, and lack of symmetry in the geometry of the specimens due to the machining of the notches by milling, which is relatively inaccurate on small scales. These aspects could be responsible for a partial overload of some areas of the specimens, where premature cracking occurred.

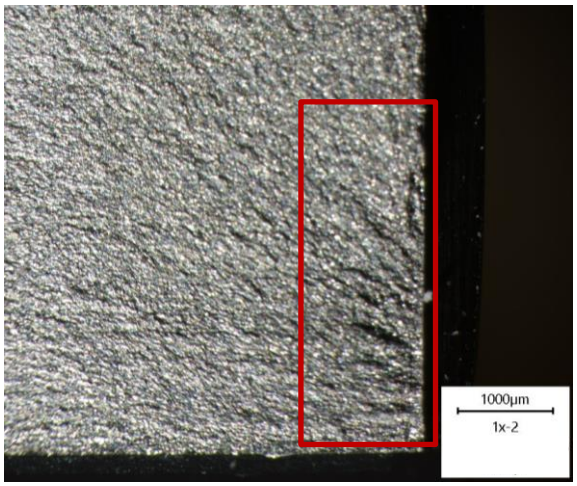

(a)

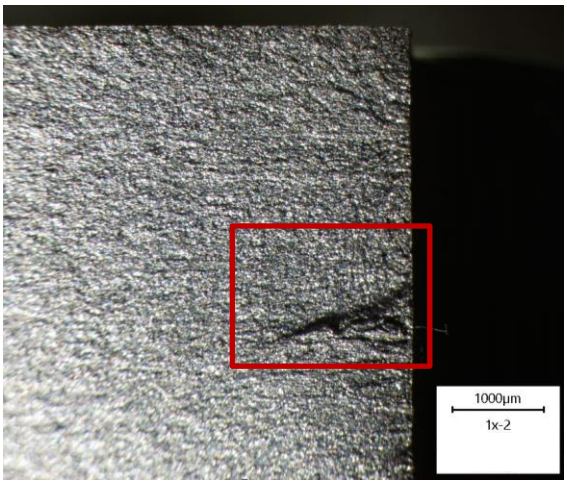

(b)

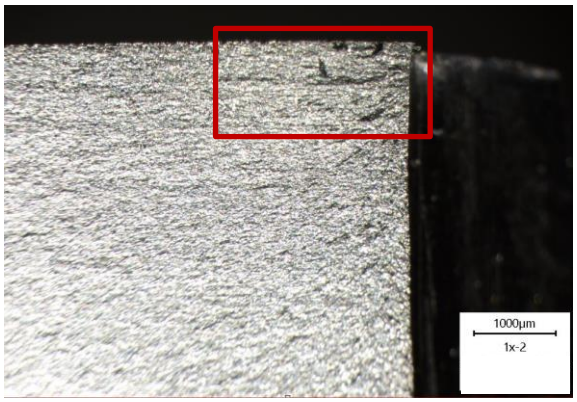

(c)

Figure 4. Fracture surfaces of the tested specimens: (a) d = 0.5 mm, (b) d = 1.0 mm, (c) d = 2.0 mm (third fracture surface adapted from [28]).

4. Conclusions and future developments

This work investigated the axial fatigue behavior of some notched specimens made of Ti-6Al-4V not subjected to STOA in inert environment. The values of *SCF* of the tested specimens were calculated using the finite element method. The specimens were tested according to the step loading procedure. The experimental results are quite in agreement with the analysis conducted with the Haigh (modified-Goodman) diagram assuming a brittle behavior of the material and an alternating stress to failure equal to 0.7 x 0.33 x *UTS* at a fatigue life of 2 million loading cycles. The analysis of the fracture surfaces with a stereo microscope provided some preliminary information on the mechanism that led to failure the tested specimens. Further experimental tests would be useful to fully understand the fatigue behavior of Ti-6Al-4V without the STOA treatment and to compare the fatigue strength of the untreated alloy with the treated one. The analysis of the fracture surfaces of the failed specimens at high magnification could help to clarify the failure mechanism. The application of strain gauges on the specimens to monitor the stress state in the specimen during the experimental tests could enable the identification of eventual parasitic stresses.

Acknowledgments

The authors wish to acknowledge NEVI S.r.l. for the machining of the specimens.

References

[1] Zheng C, Wang F, Cheng X, Liu J, Fu K, Liu T, Zhu Z, Yang K, Peng M and Jin D 2015 *Int. J. Impact Eng.* **85** 161-169
[2] Lütjering G and Williams J C 2007 Alpha + Beta Alloys *Titanium Engineering Materials* Springer (Berlin) pp 203–258
[3] Peirs J, Tirry W, Amin-Ahmadi B, Coghe F, Verleysen P, Rabet L, Schryvers D and Degrieck J 2013 *Mater. Charact.* **75** 79-92
[4] Kakogiannis D, Verleysen P, Belkassem B, Coghe F and Rabet T 2018 *Int. J. Impact Eng.* **119** 1-13
[5] Altenberger I, Nalla R K, Sano Y, Wagner L and Ritchie R O 2012 *Int. J. Fatigue* **44** 292–302
[6] Baragetti S, Guagliano M and Vergani L 2000 *Int. J. Mater. Prod. Technol* **15** 91–103
[7] Baragetti S and Tordini F 2007 *Int. J. Fatigue* **29** 1832–1838
[8] Lewandowski J J and Seifi M 2016 *Annu. Rev. Mater. Res.* **46** 151–186
[9] Nesládek M, Matušů M, Papuga J, Mžourek M and Roudnická M 2022 Some Observation Concerning Fatigue Response of Additively Manufactured Specimens from Ti-6Al-4V *Fatigue and Fracture of Mateials and Structures ed* (vol 24) eds G Lesiuk, S Duda, J.A.F.O. Correia, A.M.P. De Jesus (Cham: Springer) pp 251-358
[10] Arcieri E V, Baragetti S and Božić Ž 2021 *Procedia Struct. Integr.* **31** 22-27
[11] Nicholas T 2006 Foreign Object Damage *High Cycle Fatigue* Elsevier Science Ltd (Oxford) pp 322–376
[12] Baragetti S, Cavalleri S and Tordini F 2012 *Key Eng. Mater.* **488-489** 502-505
[13] Baragetti S 2013 *Surf. Interface Anal.* **45** 1654-1658
[14] Baragetti S, Foglia C and Gerosa R 2012 *Key Eng. Mater.* **525–526** 505–508
[15] Baragetti S 2014 *Mater.* **7** 4349-4366
[16] Baragetti S and Villa F 2014 *Frat. ed Integrita Strutt.* **30** 84–94
[17] Baragetti S and Arcieri E V 2018 *Int. J. Fatigue* **112** 301-307
[18] Baragetti S, Borzini E and Arcieri E V 2018 *Procedia Struct. Integr.* **12** 173-182
[19] Baragetti S, Borzini E and Arcieri E V 2019 *Corr. Rev.*
[20] Muttoni S and Legrenzi N 2022 Progettazione di telai per veicoli ibridi e caratterizzazione di materiali ad alto rapporto resistenza / massa (leghe di titanio e alluminio) (bachelor thesis)
[21] Baragetti S and Baryshnikov A 2001 *J. Mech. Design* **123** 456-463
[22] Srinivasan N, Bhaskar L K, Kumar R and Baragetti S 2018 *Mater. Des.* **160** 303-312
[23] Baragetti S 2006 *Meccanica* **41** 443-458

[24] Baragetti S and Arcieri E V 2019 *Procedia Struct. Integr.* **24** 91-100
[25] Yan G, Crivoi A, Sun Y, Maharjan N, Song X, Li F and Tan M J 2018 *Manuf. Process.* **32** 763-772
[26] Baragetti S and Medolago A 2013 *Key Eng Mater.* **525-526** 501-504
[27] ABAQUS, ABAQUS Documentation, Dassault Systèmes, Providence, RI, USA, 2017
[28] Arcieri E V and Baragetti S 2022 *AIP Conf. Proc*. (submitted)
[29] Nicholas T 2002 *Fatigue Fract. Eng. Mater. Struct.* **25** 861-869
[30] Locati L 1955 *Metall. Ital.* **47** 301–308
[31] Braut S, Tevčić M, Butković M, Božić Ž and Žigulić R 2021 *Procedia Struct. Integr.* **31** 33-37
[32] Schjve J 2009 Fatigue and Scatter *Fatigue of Structures and Materials* Springer (Dodrecht) pp 373-394
[33] Baragetti S and Arcieri E V 2022 *Proc. Inst. Mech. Eng, Part C* **236** 10713-10722